The early origin of Iguanodontia: new insights on the macroevolution, diversity and biogeography of the clade

FILIPPO MARIA ROTATORI[1,2, *, †], ALFIO ALESSANDRO CHIARENZA[3, *, †], FEDERICO FANTI[4], MIGUEL MORENO-AZANZA[1,2,5]

Supplementary Information

Supplementary information include:

- Maximum Parsimony sensitivity test
- Bayesian Inference sensitivity test

Supplementary figures

The supplementary figures include:

- **Figures S1-S4**: trees from sensitivity tests
- **Figures S5-S13:** strict consensus trees from Implied Weight analyses (K3-K11)
- **Figure S14**: maximum compatibility tree (MCT) of the non-clock Bayesian inference analysis.
- **Figure S15**: morphological trends within the carpus of Iguanodontia.

Maximum Parsimony sensitivity test

To test the stability of our topology, we assessed the completeness index of each taxon present in the matrix, scored as:

$$number\ of\ scored\ characters\ for\ certain\ taxon/total\ number\ of\ characters * 100$$

We then removed the taxa <30% complete and we run a tree search in TNT v 1.6 (Goloboff & Morales 2023). A heuristic search with 1000 replicates was performed, keeping 10 trees per replicate. To better explore the tree space, the trees found with the initial search were subjected to another round of Tree Bisection Reconnection (TBR). We ten calculated a strict consensus tree from the MPTs obtained. The general topology is consistent with the result presented in the manuscript and previous iteration of the this dataset (Xu *et al.* 2018; Lockwood *et al.* 2021; Rotatori *et al.* 2025).

The taxa removed are: *Dakotadon lakotaensis*, *Batyrosaurus rozhdestvenskyi*, *Magnamanus soriaensis*, *Valdosaurus canaliculatus*, *Lanzhousaurus magnidens*, *Morelladon beltrani*, *Delapparentia turolensis*, SHN Specimen, *Eousdryosaurus nanohallucis*, *Oblitosaurus bunnueli*, *Draconyx loureiroi*, *Penelopognathus weishampeli.*

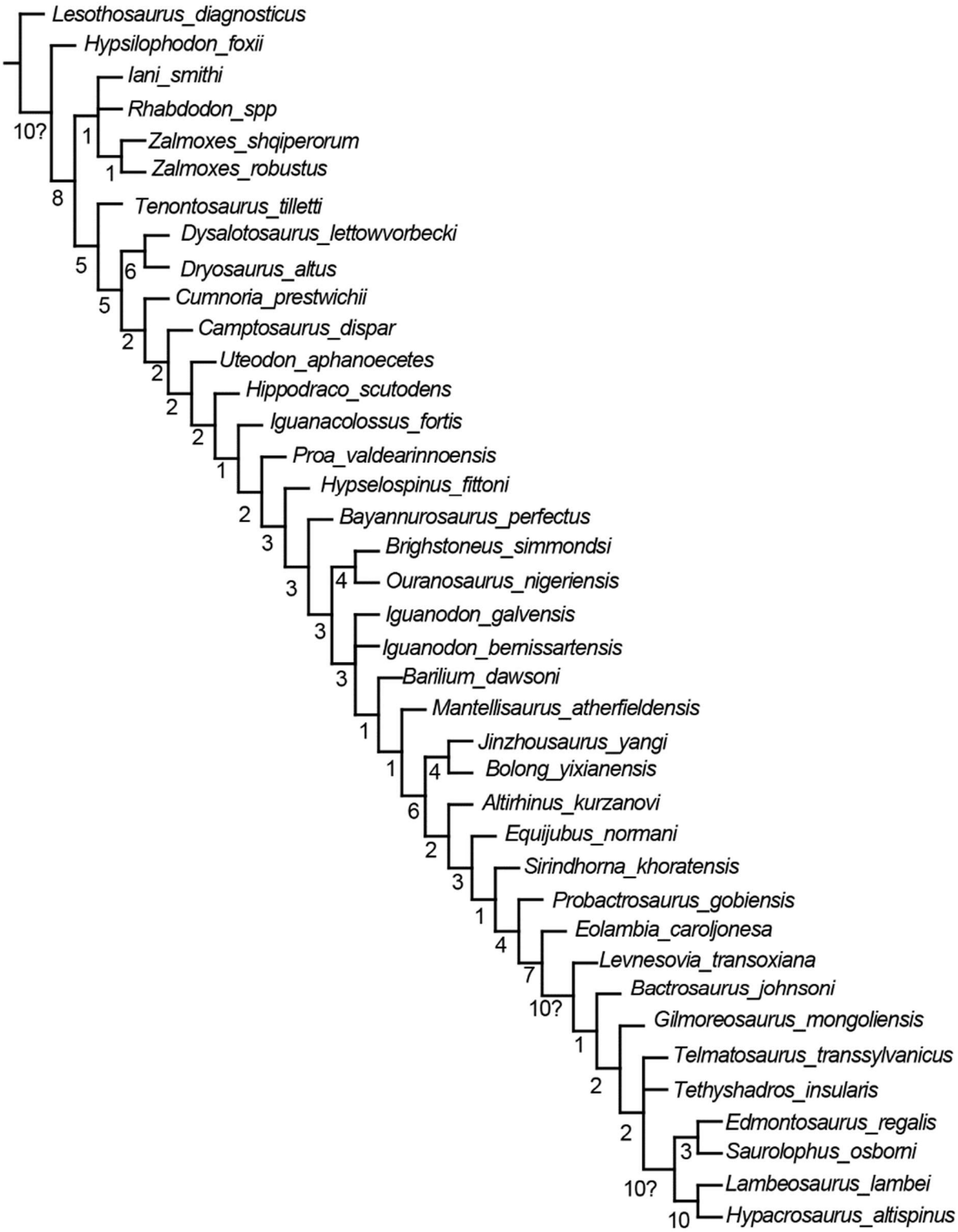

Figure S1: strict consensus tree of the sensitivity test of Maximum Parsimony. Number below branches indicate Bremer Support.

Bayesian Inference sensitivity tests

To test the robustness of our results, we performed three additional clock analyses, adopting alternative clock priors and models. We conducted one additional morphoclock analysis following Lee *et al*. (2014) and two separate Fossilised Birth–Death (FBD) model analyses (Gavryushkina *et al.* 2014). The model choice for characters and the corresponding priors were kept unchanged.

The original morphoclock analysis used tip calibrations under an Independent Gamma Rates (IGR) clock model with a normal (0.01, 0.1) clockrate prior.

In the modified morphoclock analysis, we included a soft upper bound (210–215 Ma) consistent with the stratigraphic range of Ornithischia (Baron 2019; Fonseca *et al.* 2024) . The clock-rate prior was derived from the non-clock analysis by dividing the median tree length in substitutions (from posterior trees) by the mean tree age based on the root prior distribution (7.86/215 = 0.04), following Simões *et al*.(Simões *et al.* 2020*a*, *b*). Rates were modelled under a log-normal distribution, with the mean set to the non-clock tree estimate (0.04, ln = –3.2188), and the exponent of the mean ($e^{0.04}$ = 1.040) used to provide a broad standard deviation. Two FBD analyses were also performed, both sampled under a diversity strategy to maximise the probability of modern taxon sampling (using a "dummy" taxon) and corrected to avoid the sampled-ancestor option. The first FBD analysis retained the clock priors from the initial morphoclock analysis, whereas the second adopted those from the modified morphoclock version.

Each analysis used a total of 50-80 million generations (ngen=50000000/ ngen=80000000), with a relative burn-in of 25% of the sampled trees (relburnin=yes burninfrac=0.25). The Markov chain Monte Carlo (MCMC) results were logged and sampled every 10,000 generations (printfreq=10000 samplefreq=10000), providing a balance between chain mixing and file size. Each analysis was performed using four independent runs (nruns=4), each composed of four Metropolis-coupled chains (nchains=4) with three heated chains and one cold chain, and a swap frequency of three (nswaps=3) to enhance mixing efficiency and ensure convergence among runs. These analyses were run on Mr Bayes on the online resource CIPRES, convergence was assesses analysing traces via Tracer v.1.7.1 (Rambaut *et al.* 2018).

Analysis ID	Model type	Clock model	Clock rates prior	Tree age / time calibration	Character model	Sampling strategy	Notes / References
Morphoclock 1 (original analysis)	Morphoclock (*Lee et al. 2014*)	Independent Gamma Rates (IGR)	Normal(0.01, 0.1)	Calibrated from tips	Mkv + Γ (*lset coding=variable rates=gamma*)	—	/
Morphoclock 2 (modified)	Morphoclock (*Lee et al. 2014*)	Independent Gamma Rates (IGR)	Log-normal: mean ln = –3.2188 (≈ 0.04), SD = e^0.04 = 1.040	Soft upper bound 210–215 Ma (Ornithischia; Baron 2019; Fonseca et al. 2024)	Mkv + Γ (*lset coding=variable rates=gamma*)	—	Upper soft bound on tree root age; Clock rates derived from non-clock analysis
FBD 1	Fossilised Birth–Death (*Gavryushkina et al. 2014*)	Independent Gamma Rates (IGR)	Same as Morphoclock 1 (Normal 0.01, 0.1)	Calibrated from tips	Mkv + Γ (*lset coding=variable rates=gamma*)	Diversity strategy	Sampled-ancestor option disabled; Tree root calibrated; Clock rates prior not derived from non-clock analysis
FBD 2	Fossilised Birth–Death (*Gavryushkina et al. 2014*)	Independent Gamma Rates (IGR)	Same as Morphoclock 2 (log-normal)	Soft upper bound 210–215 Ma (Ornithischia; Baron 2019; Fonseca et al. 2024)	Mkv + Γ (*lset coding=variable rates=gamma*)	Diversity strategy	Sampled-ancestor option disabled; Upper soft bound on tree root age; Clock rates derived from non-clock analysis

Table ST1: parameters of the Bayesian Inference analysis used in this manuscript

Morphoclock 2

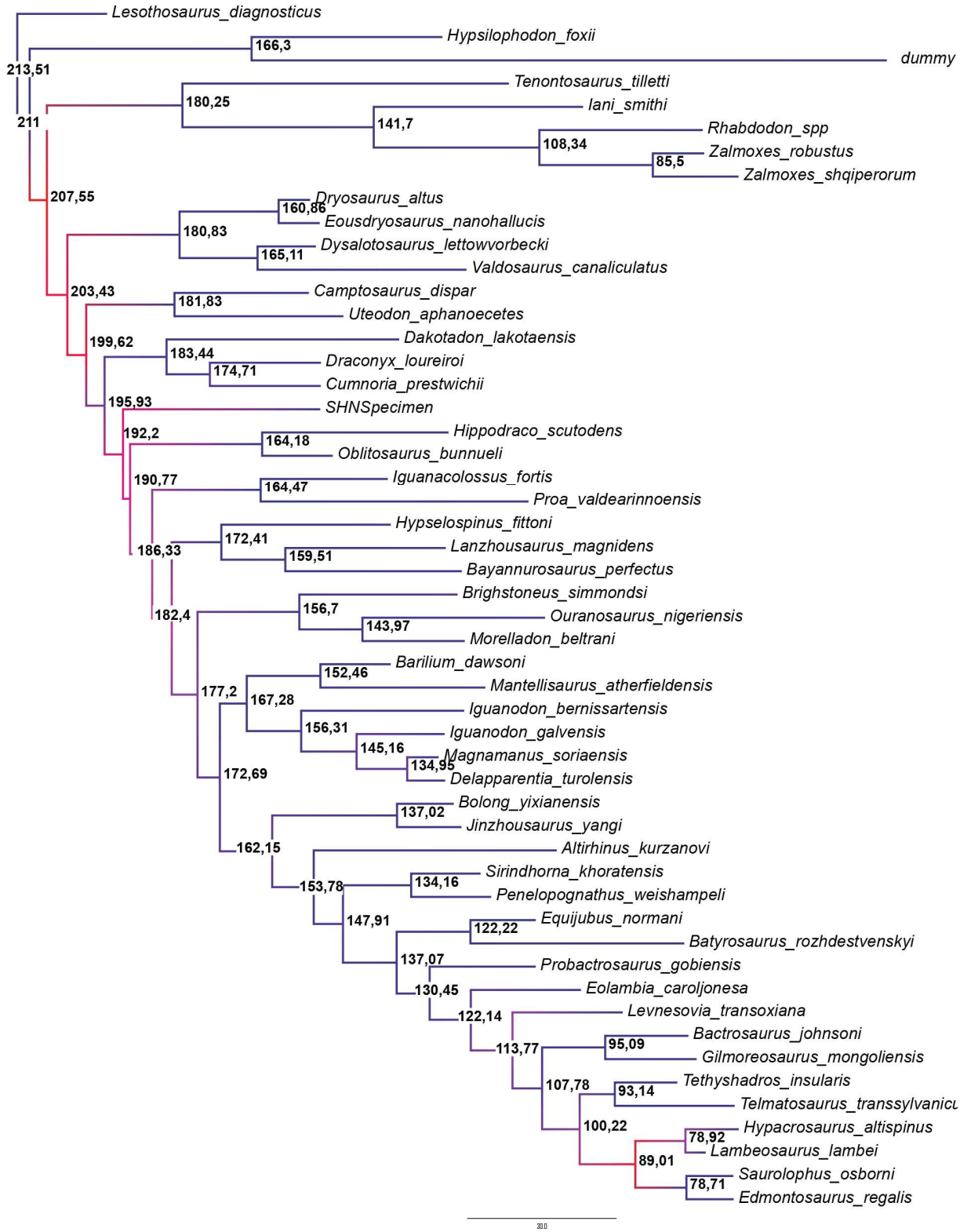

Figure S2: Maximum Compatibility Tree (MCT) of the Morphoclock 2 analysis. Numbers are divergence times in Ma.

FBD1

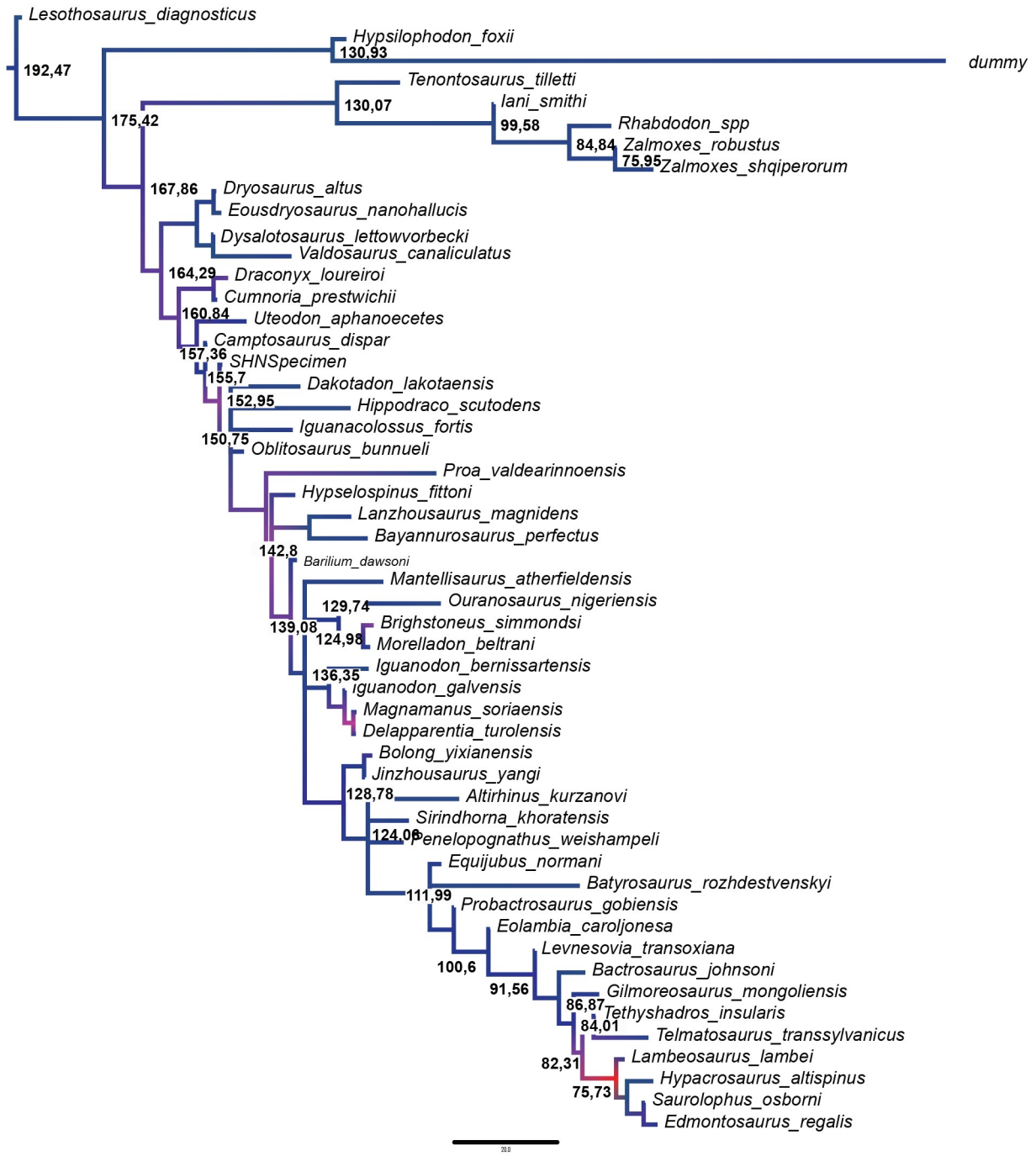

Figure S3: Maximum Compatibility Tree (MCT) of the Fossilised Birth Death Model analysis 1 (FBD1). Numbers are divergence times in Ma.

FBD2

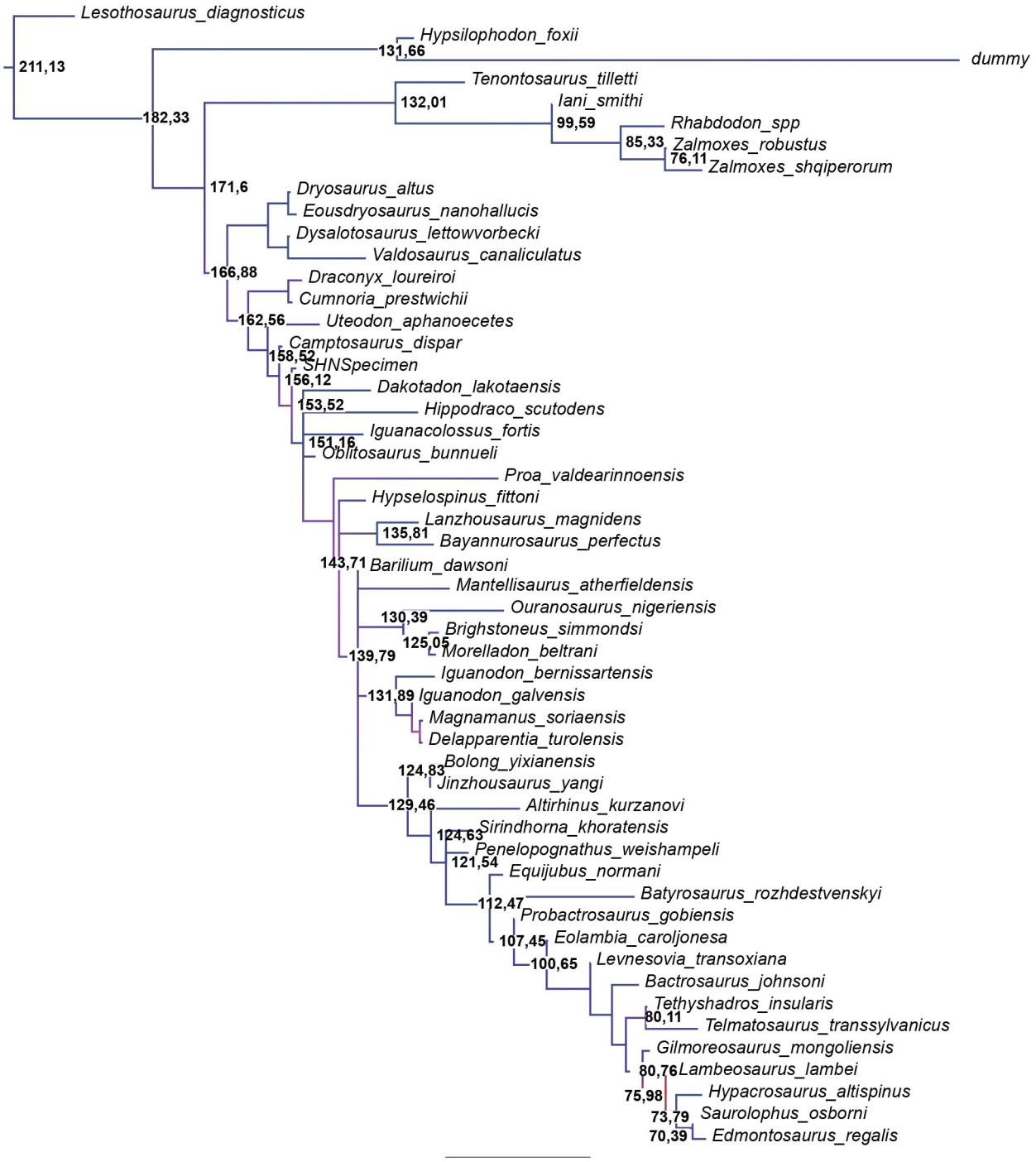

Figure S4: Maximum Compatibility Tree (MCT) of the Fossilised Birth Death Model analysis 2 (FBD3). Numbers are divergence times in Ma.

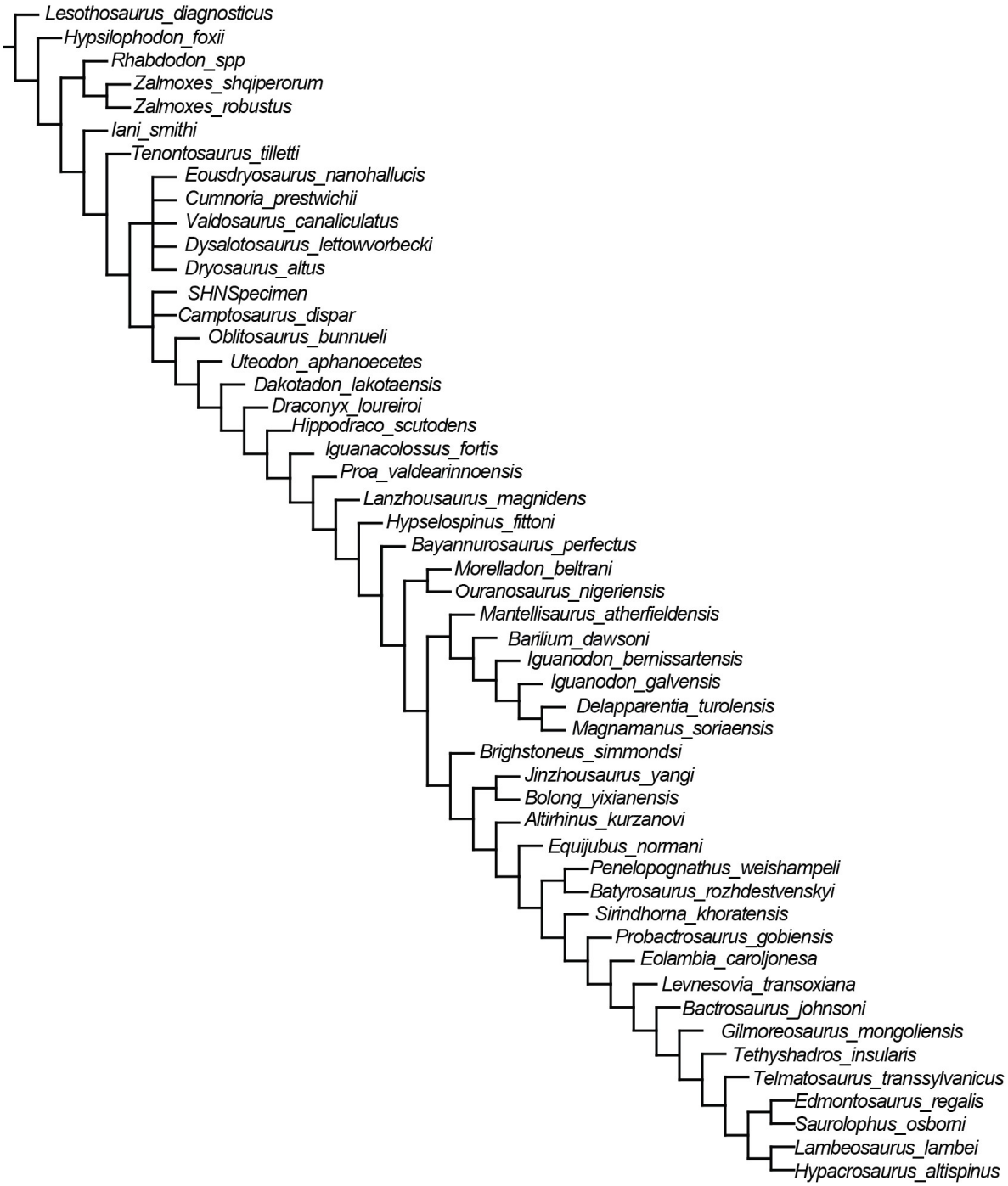

Figure S5: strict consensus tree of the implied weighting analysis (K3).

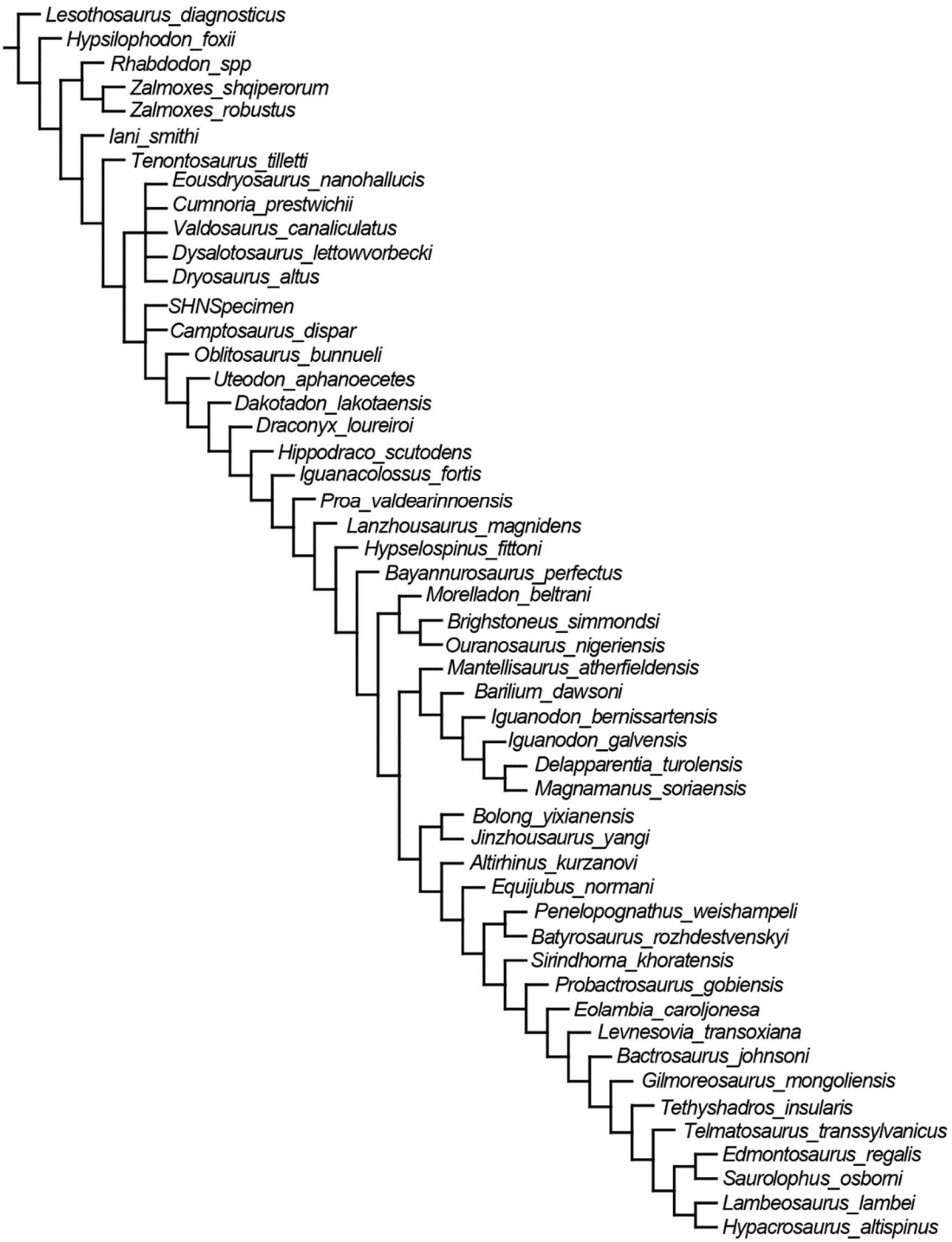

Figure S6: strict consensus tree of the implied weighting analysis (K4).

Figure S7: strict consensus tree of the implied weighting analysis (K5).

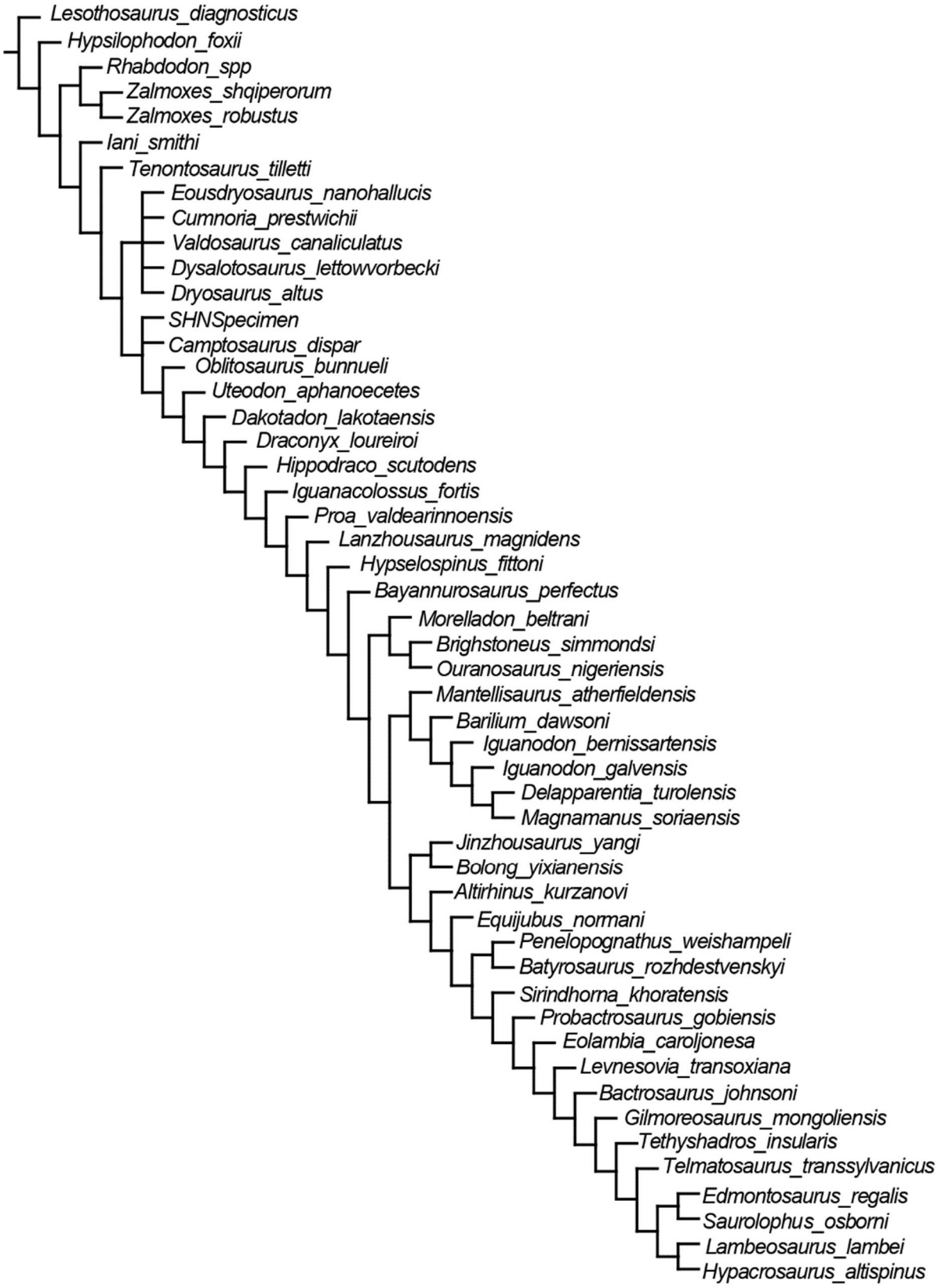

Figure S8: strict consensus tree of the implied weighting analysis (K6).

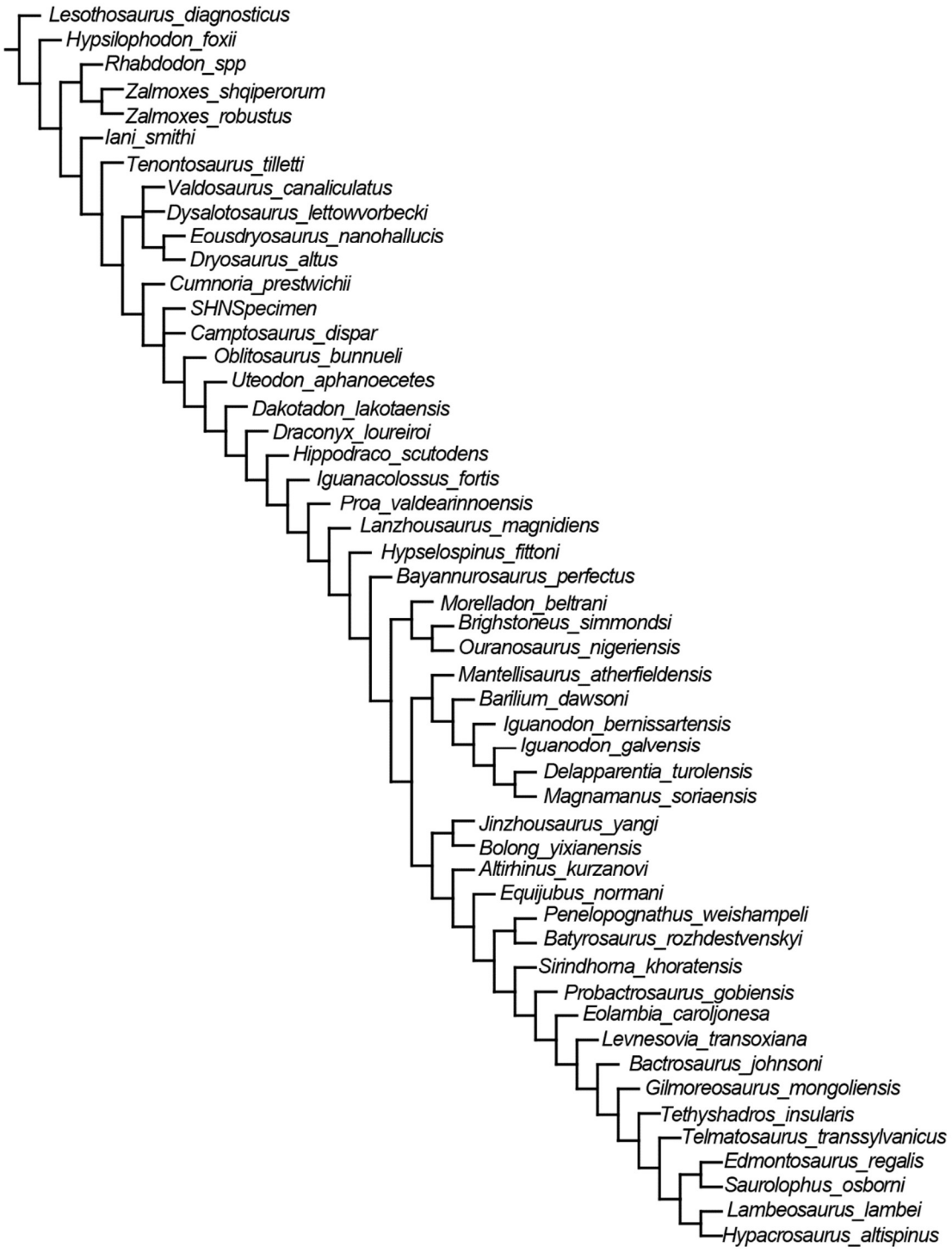

Figure S9: strict consensus tree of the implied weighting analysis (K7).

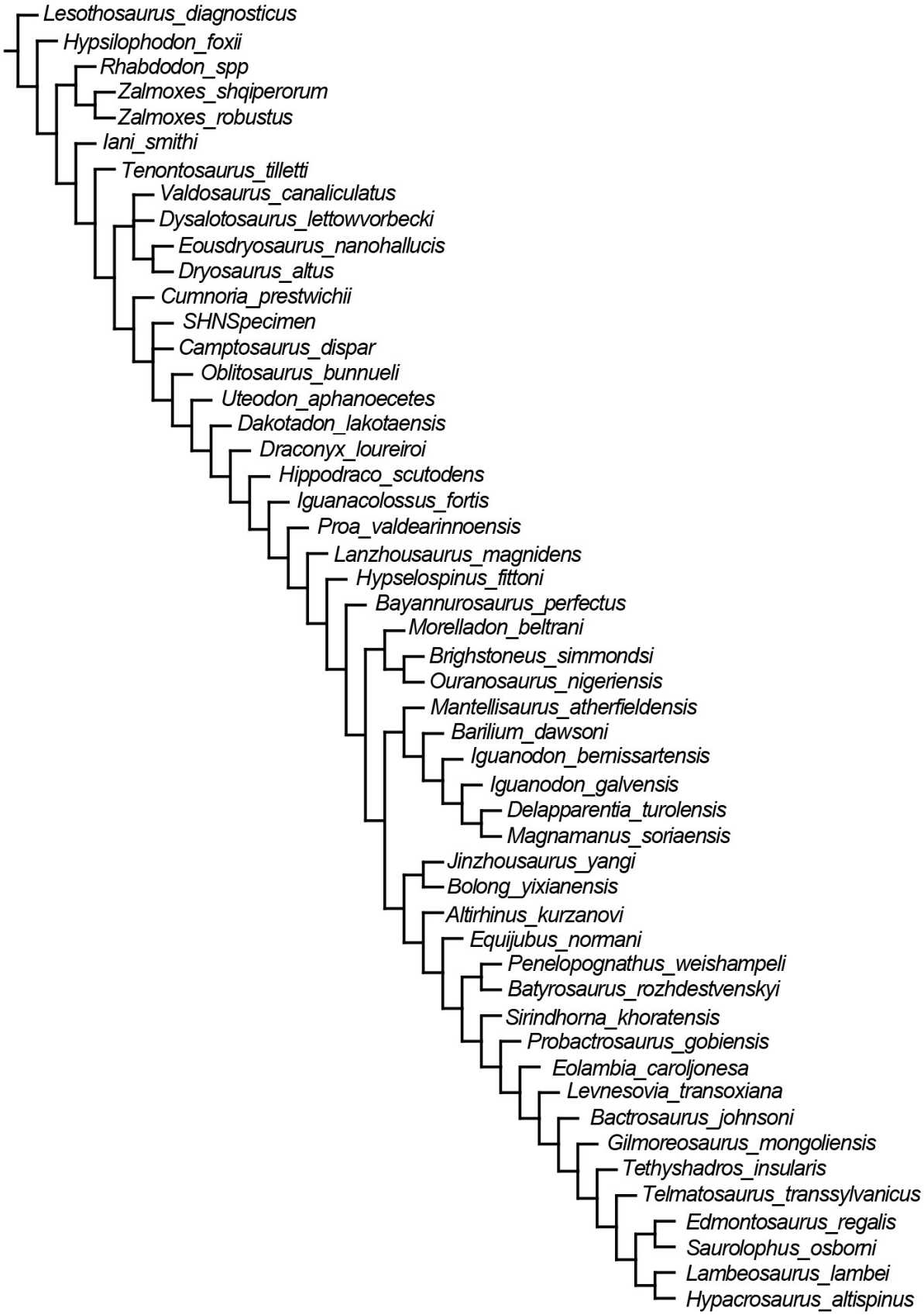

Figure S10: strict consensus tree of the implied weighting analysis (K8).

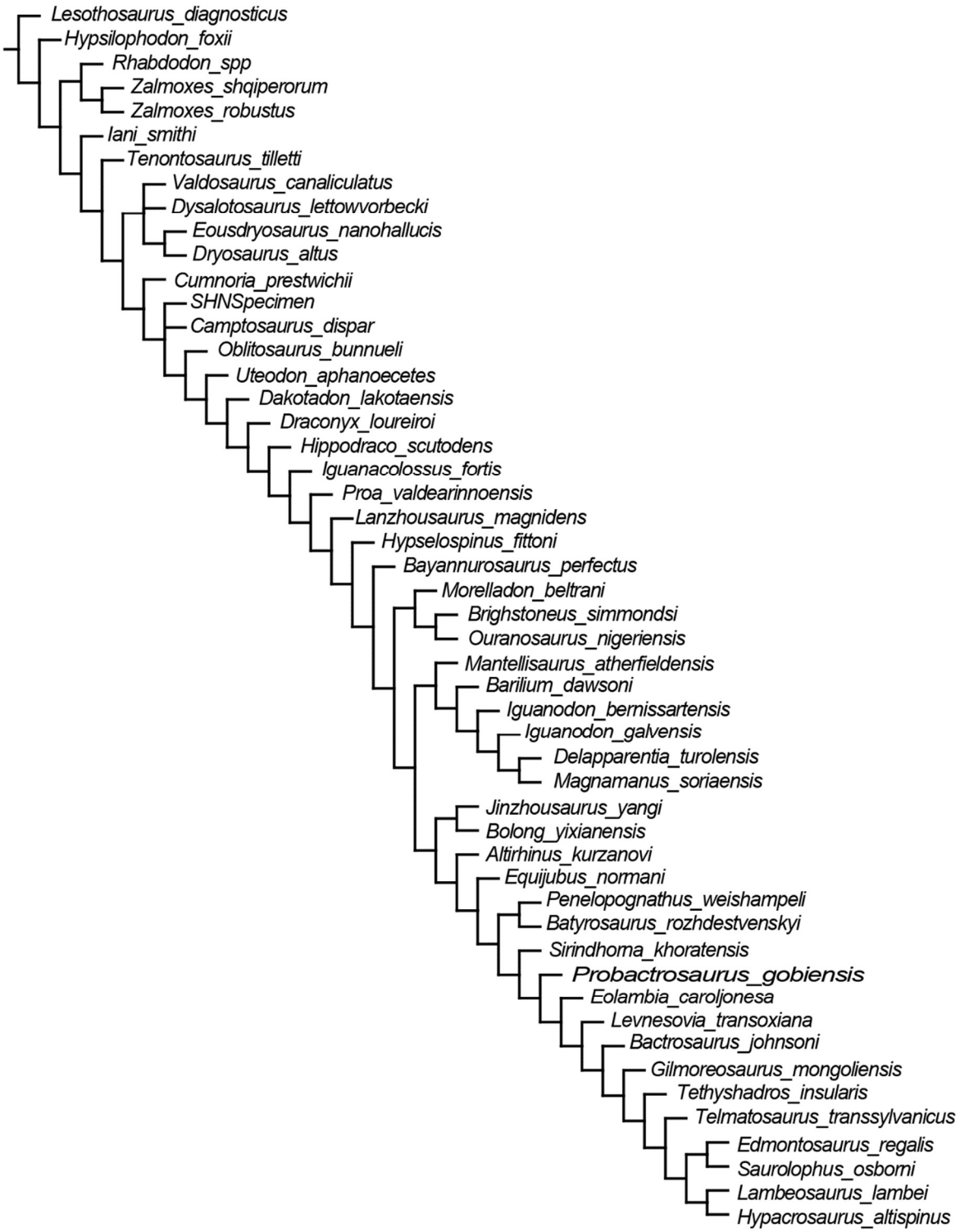

Figure S11: strict consensus tree of the implied weighting analysis (K9).

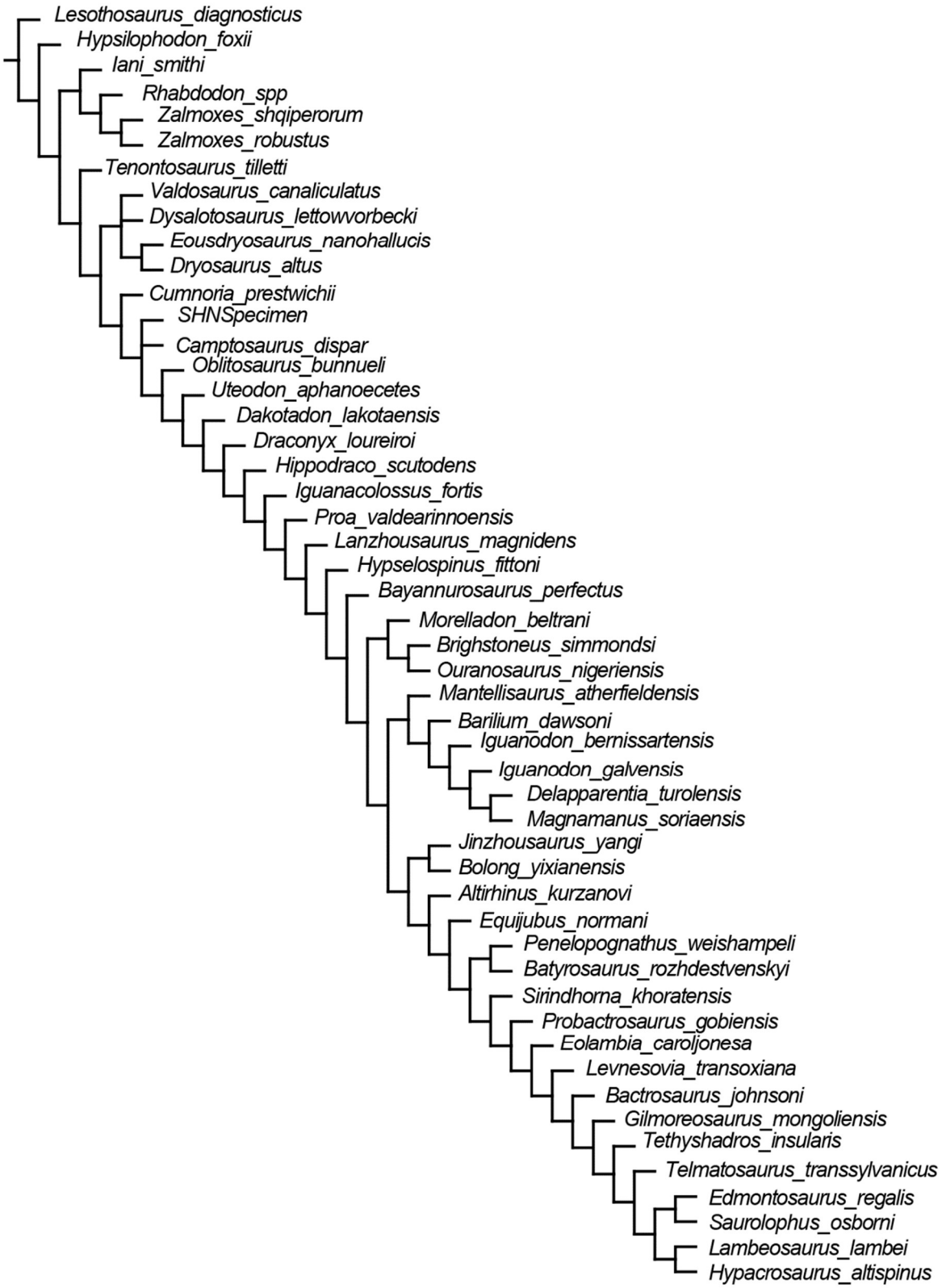

Figure S12: strict consensus tree of the implied weighting analysis (K10).

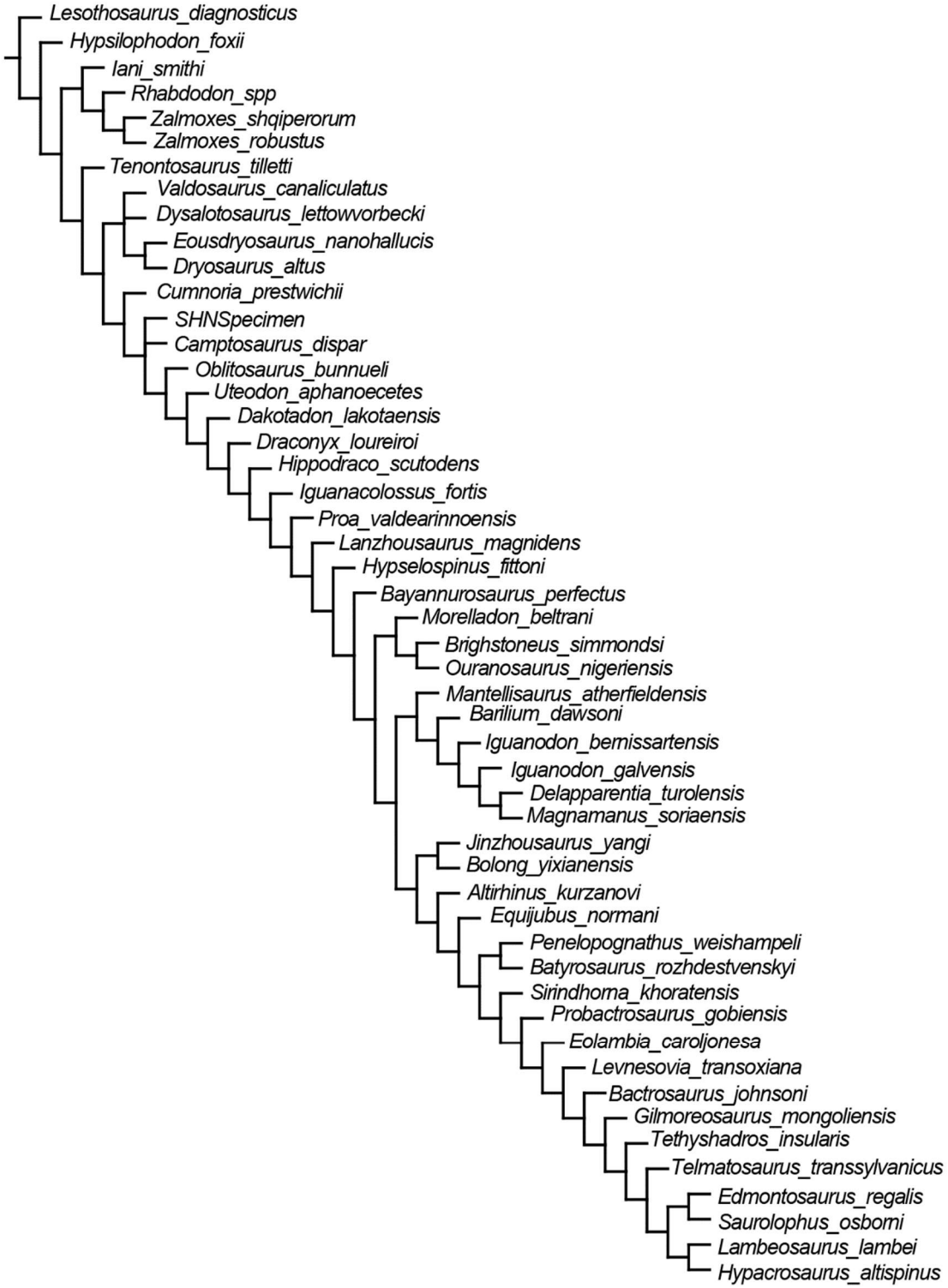

Figure S13: strict consensus tree of the implied weighting analysis (K11).

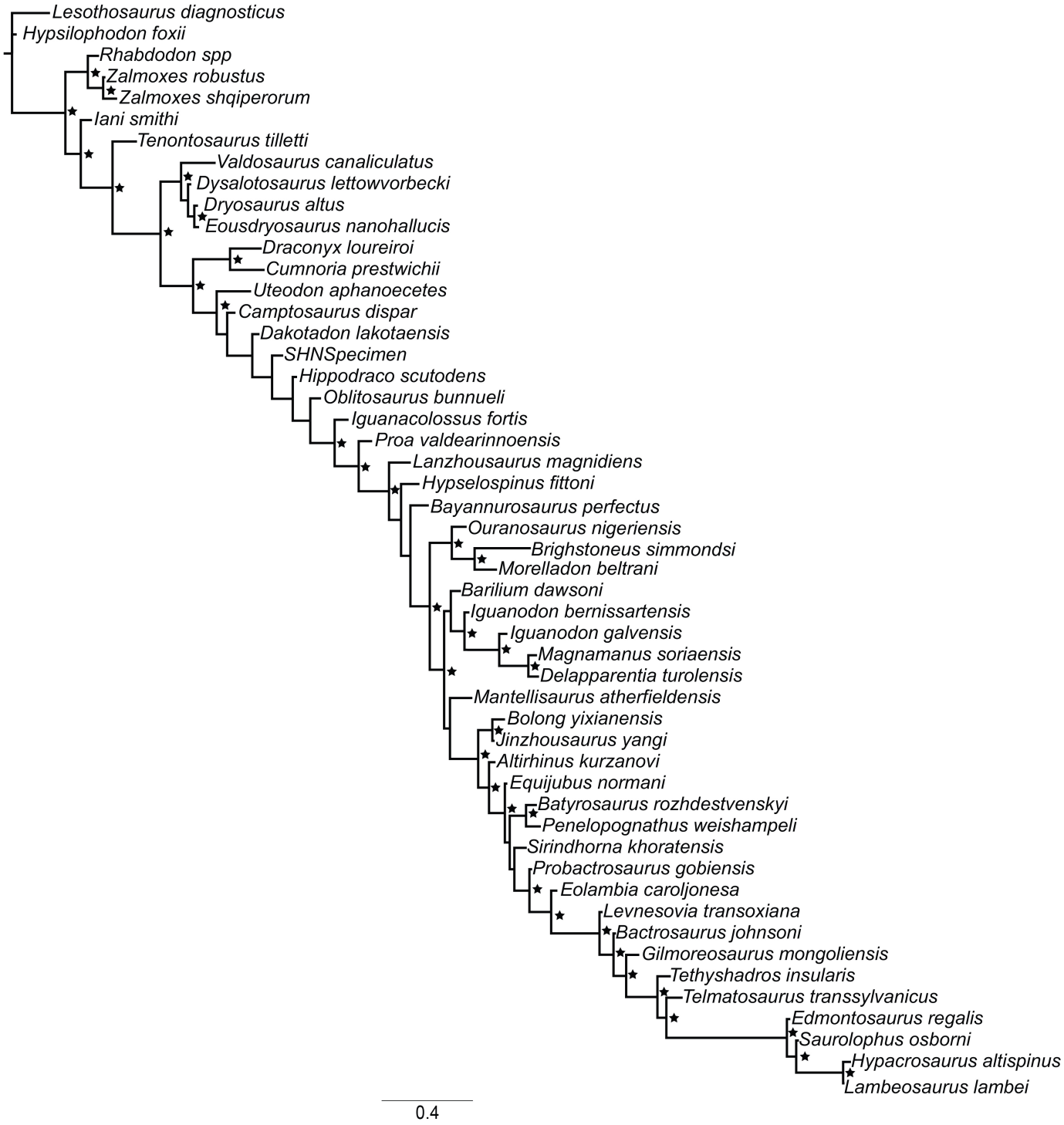

Figure S14: maximum compatibility tree (MCT) of the non-clock Bayesian analysis. The star symbols indicate posterior probability values above 50%.

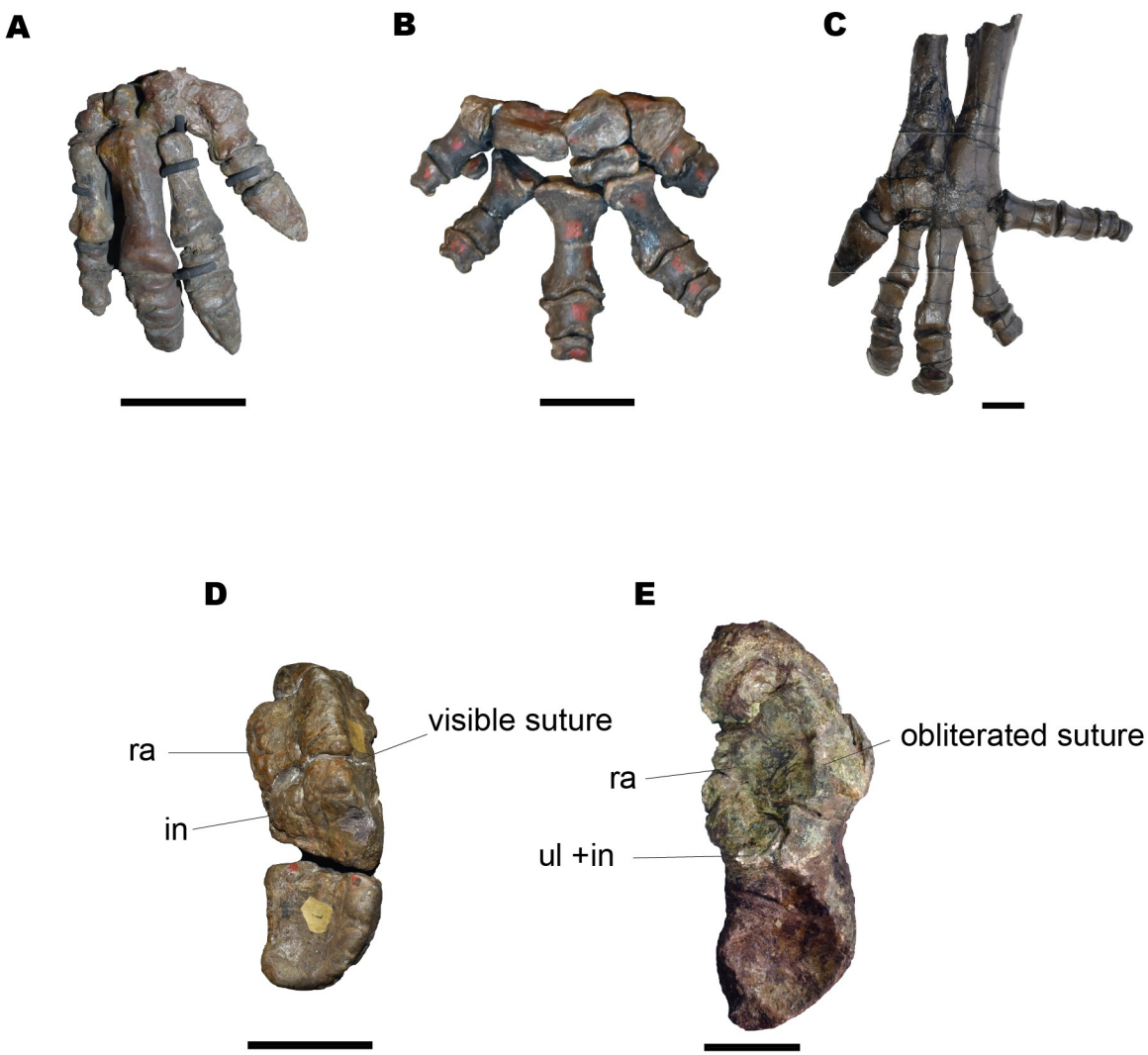

Figure S15: Examples of morphological trends within Iguanodontia. Unfused carpal elements (**A**, *Uteodon apahanoecetes* holotype, CM 11337), interlocked carpal elements (**B** *Camptosaurus dispar* holotype, YPM 1880) and fused carpus (**C**, *Iguanodon bernissartensis* RBINS 05144_01733). Degree of fusion between radiale and intermedium: suture still visible (*Camptosaurus dispar*, USNM 6001), suture obliterated (*Barilium dawsoni*, NHMUK R2357). Abbreviations: in, intermedium; ra, radiale; ul, ulnare. Scale bars: 5 cm.

References

BARON, M. G. 2019. Pisanosaurus mertii and the Triassic ornithischian crisis: could phylogeny offer a solution? *Historical Biology*, **31**, 967–981.

FONSECA, A. O., Reid ,Iain J., Venner ,Alexander, Duncan ,Ruairidh J., Garcia ,Mauricio S. and AND MÜLLER, R. T. 2024. A comprehensive phylogenetic analysis on early ornithischian evolution. *Journal of Systematic Palaeontology*, **22**, 2346577.

GAVRYUSHKINA, A., WELCH, D., STADLER, T. and DRUMMOND, A. J. 2014. Bayesian Inference of Sampled Ancestor Trees for Epidemiology and Fossil Calibration. *PLOS Computational Biology*, **10**, e1003919.

GOLOBOFF, P. A. and MORALES, M. E. 2023. TNT version 1.6, with a graphical interface for MacOS and Linux, including new routines in parallel. *Cladistics*, **39**, 144–153.

LOCKWOOD, J. A., MARTILL, D. M. and MAIDMENT, S. C. 2021. A new hadrosauriform dinosaur from the Wessex Formation, Wealden Group (Early Cretaceous), of the Isle of Wight, southern England. *Journal of Systematic Palaeontology*, **19**, 847–888.

RAMBAUT, A., DRUMMOND, A. J., XIE, D., BAELE, G. and SUCHARD, M. A. 2018. Posterior summarization in Bayesian phylogenetics using Tracer 1.7. *Systematic biology*, **67**, 901–904.

ROTATORI, F. M., ESCASO, F., CAMILO, B., BERTOZZO, F., MALAFAIA, E., MATEUS, O., MOCHO, P., ORTEGA, F. and MORENO-AZANZA, M. 2025. Evidence of large-sized ankylopollexian dinosaurs (Ornithischia: Iguanodontia) in the Upper Jurassic of Portugal. *Journal of Systematic Palaeontology*.

SIMÕES, T. R., CALDWELL, M. W. and PIERCE, S. E. 2020*a*. Sphenodontian phylogeny and the impact of model choice in Bayesian morphological clock estimates of divergence times and evolutionary rates. *BMC biology*, **18**, 1–30.

SIMÕES, T. R., VERNYGORA, O., CALDWELL, M. W. and PIERCE, S. E. 2020*b*. Megaevolutionary dynamics and the timing of evolutionary innovation in reptiles. *Nature Communications*, **11**, 3322.

XU, X., TAN, Q., GAO, Y., BAO, Z., YIN, Z., GUO, B., WANG, J., TAN, L., ZHANG, Y. and XING, H. 2018. A large-sized basal ankylopollexian from East Asia, shedding light on early biogeographic history of Iguanodontia. *Science Bulletin*, **63**, 556–563.